Transcellular Permeability of Chlorpromazine Demonstrating the Roles of Protein Binding and Membrane Partitioning

Geri A. Sawada,[1] Norman F. H. Ho,[1] Larry R. Williams,[2,3] Craig L. Barsuhn,[1] and Thomas J. Raub[1,4]

Received July 17, 1993; accepted November 28, 1993

Transcellular permeability of the neuroleptic-anesthetic chlorpromazine (CPZ) was examined using a cell type (MDCK) that forms a confluent monolayer of polarized cells resulting in distinct apical (AP) and basolateral (BL) membrane domains separated by tight junctions. Because CPZ is membrane interactive, transmonolayer flux was analyzed as two kinetic events: cell uptake from the AP donor solution and efflux into the BL side receiver. Using the rate of cell uptake in the presence of different concentrations of BSA, an intrinsic cell partition coefficient of 3700 ± 130 and an operational dissociation binding constant of 0.4 ± 0.05 m*M* were calculated. In contrast to uptake, efflux of CPZ from either the AP or the BL side of the cell monolayer was ~10^4-fold slower and was dependent upon the avidity of CPZ for the protein acceptor in the receiver solution. These results emphasized the importance of simultaneously measuring disappearance of a lipophilic molecule from the donor solution and its appearance in the receiver and demonstrated how interactions with proteins on either side of the cellular barrier influence permeability. Appearance kinetics showed that the composition of the receiving environment is critical to model a particular *in vivo* situation and implied that the intrinsic permeability of membrane-interactive molecules *in vitro* does not necessarily predict penetration beyond the initial cellular barrier *in vivo*.

KEY WORDS: biophysical model; cell culture model; chlorpromazine; permeability.

INTRODUCTION

Plasma protein binding greatly affects the ability of molecules to permeate cellular barriers, especially endothelium, and penetrate the underlying tissues. Likewise, access of lipophilic molecules to intracellular sites can be significantly restricted despite a favorable intrinsic transmembrane permeability. It was originally thought that only the unbound or free drug concentration was available for uptake by tissues. However, the validity of the free drug hypothesis has been questioned by numerous examples where tissue uptake also depends upon the fraction bound (1). Many *in vitro* methods have been devised to predict pharmacokinetic consequences of protein binding *in vivo;* however, correlations are inconclusive (2). Nevertheless, the *in vitro* assays have provided a means to understand the molecular events of drug–protein interaction and subsequent partitioning into tissues. The aspects of tissue uptake related to the partitioning of a molecule from the initial cell barrier to the underlying cells have not been well studied.

Chlorpromazine (CPZ)[5] is an aliphatic derivative of the antipsychotic phenothiazines. By nature of its unique physical-chemical properties, CPZ is also a membrane anesthetic and has been studied extensively (3). We chose CPZ as a model compound to examine the way lipophiles cross a cellular barrier. CPZ is relatively hydrophobic, with a log $PC_{(n\text{-octanol/water})} \approx 3.16$ at pH 7.4 (5.3 for the uncharged molecule), and complete ionization ($pK_a = 9.3$) in solution at pH 7.4 gives it a relatively high water solubility (4,5). In addition, CPZ is 92–99% protein bound *in vivo* and the volume of distribution in man of ~11 L/kg indicates that CPZ does partition into vascular endothelium and, presumably, underlying tissues (6). Consequently, CPZ represents a model compound for which a plethora of information is available both *in vitro* and *in vivo*.

In the current study, a recently described cell culture-based biophysical model (7) was applied to understand how CPZ passively permeates a continuous cell barrier in the presence of plasma proteins on both the donor and receiver sides. The interplay of protein binding affinity, membrane, partitioning, and solubility are compared between CPZ and previously analyzed lipophilic antioxidants U-78517F and U-74006F (7) to define what determines permeation and brain uptake.

MATERIALS AND METHODS

Materials

The low-resistance MDCK cell line was from the American Type Culture Collection (Rockville, MD) and was maintained in culture as described previously (7). The Transwell filter inserts (24.3-mm diameter or 4.71 cm^2, 0.4-μm pore size) were from Costar (Cambridge, MA). BSA fraction V, chlorpromazine HCl, and α_1-acid glycoprotein (α_1-AGP) were from Sigma Chemical Co. (St. Louis, MO). Solvable, Protosol, D-[1-^{14}C]mannitol (55 mCi/mmol), *N*-[1-^{14}C]butanol (1.7 mCi/mmol), and [benzene ring-^{3}H]CPZ hydrochloride (30 Ci/mmol, 355.3 Da) were from Dupont NEN Research Products (Boston, MA). [^{3}H]CPZ in 100% ethanol at 1 mCi/mL was stored under nitrogen gas at −20°C in the dark to minimize oxidation/degradation. [^{3}H]Dextran (423 mCi/g) was from Amersham Corp. (Arlington Heights, IL). Hank's balanced salt solution (HBSS) was from GIBCO-BRL (Grand Island, NY), and 4-(2-hydroxyethyl)-1-piper-

[1] Drug Delivery Systems Research.

[2] Central Nervous Systems Research, Upjohn Laboratories, The Upjohn Company, Kalamazoo, Michigan 49007.

[3] Present address: Neurobiology, Amgen, Inc., Thousand Oaks, California.

[4] To whom correspondence should be addressed at Upjohn Laboratories, The Upjohn Company, 301 Henrietta Street, Kalamazoo, Michigan 49007.

[5] *Abbreviations used:* α_1-AGP, α_1-acid glycoprotein; AP, apical; BBB, blood–brain barrier; BL, basolateral; BSA, bovine serum albumin; BUI, brain uptake index; CMF-PBS, calcium- and magnesium-free phosphate-buffered saline; CPZ, chlorpromazine HCl; HBSS, Hank's balanced salt solution; HEPES, 4-(2-hydroxyethyl)-1-piperazineethanesulfonic acid; LCS, liquid scintillation counting; MDCK, Madin–Darby canine kidney; TER, transepithelial electrical resistance.

0724-8741/94/0500-0665$07.00/0

azineethanesulfonic acid (HEPES) was from Boehringer Mannheim Corp. (Indianapolis, IN). Ultima Gold scintillation fluid was from Packard (Meriden, CT).

Flux Experiments

MDCK cells were seeded onto sterile Transwell polycarbonate membrane inserts at a density of 50,000 cells/cm^2. Cells were used for experiments on day 5 or 6 after measuring the transepithelial electrical resistance (TER) of the cell monolayers (8). The cells were rinsed for 20 min with HBSS containing 10 m*M* HEPES, pH 7.4 (HBSS-HEPES), and then the apical (AP)-side (donor) chamber solution was replaced with 3% BSA in HBSS-HEPES. The basolateral (BL)-side (receiver) chamber contained either 0.1, 0.5, or 3% (w/v) BSA or 0.1% (w/v) α_1-AGP in HBSS-HEPES. After equilibration for 20 min at 37°C, the donor chambers received 1.5 mL [^{3}H]CPZ at 0.25 μCi/mL (≈3 μ*M* CPZ) in 3% BSA–HBSS-HEPES immediately after passage through a 0.2-μm pore-size filter. All incubations were performed in triplicate at 37°C with continuous mixing by nutation (Nutator, Clay Adams, Parsippany, NJ). The cell inserts were transferred to 2.5 mL fresh BSA buffer at each time point to maintain sink conditions in the receiver. Both donor (10 μL) and receiver (500 μL) aliquots were collected at regular time intervals for the duration of the experiment. At the end of the experiment the cell inserts were rinsed three times with ice-cold calcium- and magnesium-free phospate-buffered saline (CMF-PBS). The filter containing the cells was cut from the holder with a scalpel and solubilized in a glass scintillation vial with 1 mL Protosol. The radioactivity of all samples was measured in 10 mL Ultima Gold scintillation fluid by liquid scintillation counting (LSC).

Uptake Experiments

MDCK cells were plated at a density of 20,000 cells/cm^2 in plastic six-well culture dishes and used between day 5 and day 7. All incubations were performed in triplicate at 37°C with mixing as described above. The cells were washed for 20 min with HBSS-HEPES and the wash buffer was replaced with 1 mL HBSS-HEPES containing 0.1, 0.5, 1, 2, or 3% (w/v) BSA. After equilibrating for 15–20 min, the BSA buffer was replaced with fresh BSA buffer containing 0.25 μCi/mL[^{3}H]CPZ, and 10-μL samples were taken. At the end of the experiment (t = 60 min), the cells were rinsed three times with ice-cold CMF-PBS and solubilized with 1 mL Solvable for 15 min to measure cell-associated radioactivity by LSC.

Efflux Experiments

Plastic-grown cells were used to measure efflux from cells through the AP membrane. MDCK cell monolayers were allowed to accumulate [^{3}H]CPZ for 60 min or until steady-state equilibrium was reached as described for uptake experiments. The donor solutions were removed and the amount of radioactivity remaining was measured to calculate the amount accumulated by the cells. To measure efflux of [^{3}H]CPZ, each well contained 1 mL of the appropriate BSA buffer and the entire solution was carefully removed every 30 min for 3 hr and replaced with fresh BSA buffer to maintain sink conditions. At the end of the experiment the amount of radioactivity remaining cell associated was measured.

Efflux of [^{3}H]CPZ from the BL membrane was also studied. Filter-grown cells were incubated for 60 min with 0.25 μCi/mL [^{3}H]CPZ in HBSS-HEPES–3% BSA in the donor compartment only and the amount accumulated by the cell monolayer was measured as described above. To isolate efflux from the BL membrane, the AP side solution was removed, leaving a thin film to prevent drying. Sampling was done as described for flux experiments. After 4 hr, the cells were rinsed and the amount of radioactivity remaining cell associated was measured.

Data Analysis

Quantification of transport parameters in transmonolayer flux studies as a function of protein binding with BSA and α_1-AGP was achieved using the following modification of the biophysical model described in detail elsewhere (7). The rate of disappearance of [^{3}H]CPZ from the donor solution is

$$\frac{dC_D}{dt} = -\alpha C_D + (\alpha\beta + \gamma)\left[C_D(0) - C_D - \left(\frac{V_R}{V_D}\right) C_R\right] \quad (1)$$

and the rate of appearance in the receiver sink is

$$\frac{dC_R}{dt} = \gamma\left(\frac{V_D}{V_R}\right)\left[C_D(0) - C_D - \left(\frac{V_R}{V_D}\right) C_R\right] \quad (2)$$

where the apical uptake (α) and basolateral efflux (γ) rate constants and the partition parameter (β) are

$$\alpha = \frac{AP_e}{V}, \quad \text{min}^{-1} \quad (3)$$

$$\beta = \frac{V}{V_{cell}K}, \quad \text{dimensionless} \quad (4)$$

$$\gamma = \frac{AP'_{bl}}{V_{cell}}, \quad \text{min}^{-1} \quad (5)$$

$$P'_{bl} = \frac{1}{(1/\epsilon P_{bl}) + (1/P_F) + (1/P_{ABL})} \quad (6)$$

and C_D and C_R are the total concentration (free drug and protein bound drug) in the donor solution of volume V_D and the receiver solution of volume V_R, respectively; V_{cell} is the volume of the cell monolayer using an average cell height of 7 μm (8); A is the cross-sectional area (4.71 cm^2); and ϵ is the porosity of the filter (0.15). The effective uptake permeability coefficient (P_e) for the AP membrane partition coefficient (K) are functions of protein concentration. The permeability coefficients of the BL membrane *per se*, filter support, and aqueous boundary layer on the filter side are P_{bl}, P_F, and P_{ABL}, respectively. The initial boundary conditions are $C_D = C_D(0)$ and $C_R = 0$. After applying data on the change in amounts of CPZ in the donor and receiver with time to the Laplace transforms of Eqs. (1) and (2), the inverse of the simultaneous transformed equations was numerically calculated for best estimates of α, β, and γ with LAPLACE (Mi-

croMath Scientific Software, Inc., Salt Lake City, UT). This approach provided greater latitude in analyzing a range of disappearance and appearance kinetic profiles than the restricted approach used previously (7).

For uptake and efflux kinetics at the AP membrane of cells grown on plastic dishes and efflux kinetics from the BL membrane of filter-grown cells, the data were plotted and analyzed by theoretical models (7) using nonlinear least-squares curve fitting (9). All radioactivity was accounted for in each experiment to ensure that mass balance was obtained.

Brain Uptake Index

First-pass extraction of radiolabeled drug in brain was measured using the brain uptake index (BUI) method of Oldendorf (10). A 200-μL bolus of HBSS containing 3% (w/v) BSA, 2 μCi of [^{3}H]CPZ (24 μ*M*), and 0.5 μCi of the reference compound [^{14}C]butanol was injected rapidly into the left common carotid artery of anesthetized 300 to 350-g male albino Sprague-Dawley rats. The amount of [^{3}H]CPZ extracted was calculated as described elsewhere (7,10) using 0.81 as the extraction efficiency for *n*-butanol (11).

Reverse-Phase HPLC

To confirm that [^{3}H]CPZ was pure and did not contain appreciable amounts of [^{3}H]$_2$O, and that metabolism and/or chemical degradation had not occurred during the course of these experiments, cell monolayers on plastic were incubated with [^{3}H]CPZ for up to 3 hr. Donor solutions and organic solvent extracts (12) of the cells were subjected to reverse-phase HPLC using a standard C-18 column with a mobile phase consisting of 60% acetonitrile, 40% H_2O, 0.02% trifluoroacetic acid, and 0.02% dimethyloctylamine. Elution was isocratic at 1 mL/min and the output was monitored using a Radiometric Instruments Flo-One Beta radioactive flow detector.

RESULTS

Cells seeded onto plastic dishes formed a continuous monolayer within 4–5 days. The integrity of cell monolayers grown on the polycarbonate membrane inserts was determined to be maximal after day 4 by using TER measurements. Although TER measurements were not made on every monolayer for every experiment, intermittent TER measurements made throughout the study were found to be consistently ~200 $\Omega \cdot cm^2$. It was shown previously that MDCK monolayers with comparable TER values prevent appreciable paracellular leakage of membrane-impermeant, hydrophilic solutes of >300 Da (7,8); therefore, transmonolayer leakage of the CPZ–protein complex was negligible. To determine if CPZ (Fig. 1) adversely affected monolayer integrity, we simultaneously measured the AP-to-BL fluxes of [^{14}C]mannitol and [^{3}H]dextran (70 kD) with donor concentrations of 30 μ*M* CPZ or 10-fold greater than the amounts used in the kinetic studies. CPZ had no effect on transmonolayer flux of either of these extracellular solutes.

We also showed that 94–98% of the radioactivity in the donor and receiver solutions was authentic CPZ as confirmed by simultaneous UV detection of unlabeled CPZ. Of the remaining 2–6% radioactivity, the majority was most likely [^{3}H]$_2$O since it eluted with the solvent front. In aged samples of CPZ containing 10% [^{3}H]$_2$O, transmonolayer permeability coefficients for CPZ were unaffected. After 3 hr in the presence of cells, there was no apparent loss of CPZ in either cell extracts or donor solutions by metabolism or degradation. Under these conditions, ~80% of the radioactivity in the donor at time 0 became cell associated and 98.8 ± 0.1% was extracted in the organic phase, independent of the time of incubation. During this time the putative [^{3}H]$_2$O increased to only 5.0 to 7.5% of the $M_D(0)$. These results confirmed that chemical degradation or cellular metabolism was negligible and that the ensuing kinetic studies represented native CPZ.

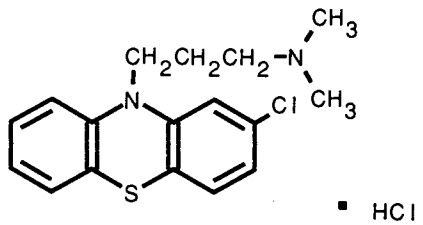

Fig. 1. The chemical structure of chlorpromazine HCl (CPZ).

Transcellular Flux

The effects of protein binding on transcellular permeability of CPZ were determined by measuring both its rate of disappearance from the AP donor solution and its rate of appearance in the BL receiver solution. The concentrations of [^{3}H]CPZ and BSA (3%) in the donor solutions were held constant, while the BSA concentration in the receiver was either 0.5 or 3.0%. There was a marked difference between the disappearance and the appearance kinetics (Fig. 2). The magnitude of these P_e values appeared to be consistent with diffusion of BSA-bound and free CPZ species across the aqueous boundary layer, which is the rate-determining step (7). Loss of CPZ from the donor solution represented partitioning into the cell monolayer and this was confirmed by mass balance. The amount of radioactivity associated with the cell at the end of the experiment was 65–85% of $M_D(0)$, depending upon the BSA concentration. It was found that <12% of $M_D(0)$ was adsorbed to the plastic surfaces and the filter by harvesting the cells with trypsin, rinsing the filter insert with 100% methanol, and measuring the amount of radioactivity recovered. These data were corrected for an 86 ± 4% efficiency of cell removal by trypsin (7).

Appearance P_e values were ~10^4-fold slower than the disappearance P_e values and the kinetics were linear with time (Fig. 2). The appearance kinetics were slightly dependent upon the concentration of BSA in the receiver solution and this had no effect upon the initial rate of disappearance. Therefore, these two events were essentially independent kinetic processes. This independence was demonstrated further by increasing the rate of appearance in the receiver by using an acceptor protein with a higher binding affinity for CPZ. α_1-AGP is a plasma protein that avidly binds most lipophilic cations, including CPZ (13). Figure 2 shows that 0.1% α_1-AGP in the receiver solution resulted in a 14-fold increase in appearance P_e compared with 0.1% BSA. De-

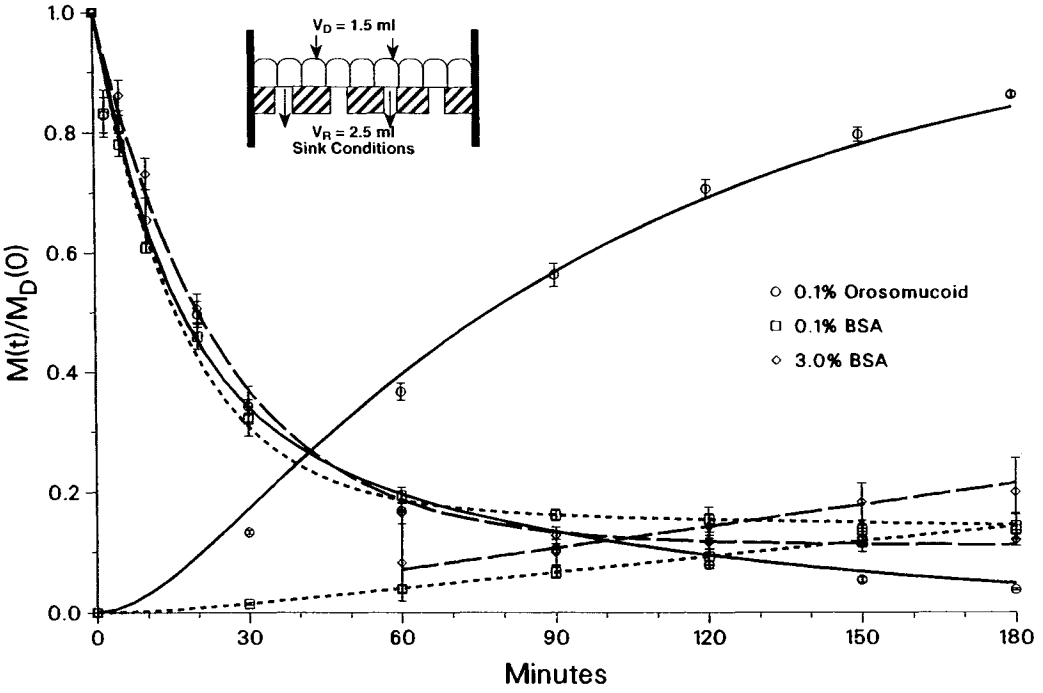

Fig. 2. Transmonolayer flux of [^{3}H]CPZ as a function of BSA or α_1-AGP in the receiver and donor. The assay was performed as described under Materials and Methods with 3% (w/v) BSA in the donor and 0.1 or 3% (w/v) protein in the receiver. The mass of CPZ in the donor (M_D) and receiver (M_R) at each time was calculated as a fraction of the mass in the donor at $t = 0$ [$M_D(0)$] and the cumulative fraction was plotted as a function of time at 37°C. Standard deviations ($n = 3$) were <5% of the mean. Mass balance was ~100%.

spite this marked increase in appearance kinetics, the initially rapid rate of disappearance was not affected, further showing that uptake was aqueous boundary layer controlled. Unlike BSA, α_1-AGP did show an effect upon the quasi-equilibrium of the disappearance kinetics after 60 min (Fig. 2). Since α_1-AGP was efficiently depleting the cell monolayer of CPZ at a rate much faster than replenishment from the donor, a relatively large net concentration gradient was maintained; hence, the quasi-equilibrium state observed with BSA was not attained.

Uptake Kinetics

To focus on the roles of protein binding and transfer of CPZ between the aqueous phase and the AP membrane, uptake kinetic experiments were conducted with cells cultured on a plastic dish. The CPZ concentration was kept constant and the BSA concentration was varied from 0 to 5% (w/v) or from 0 to 0.8 m*M* (BSA, 66 kD). Both the exponential uptake kinetics and the equilibrium levels that were cell associated decreased proportionately to increased BSA concentration (Fig. 3). Using nonlinear least-squares curve fitting per the biophysical-kinetic model described, the effective permeabilities (P_e) and the apparent cell/BSA buffer partition coefficients (K) at pH 7.4 were calculated. The uptake P_e and K values were found to be weakly influenced by BSA concentration (Fig. 4). These uptake P_e values were ~2-fold faster than the uptake P_e values measured from the transmonolayer flux experiments because the hydrodynamics were different. The Transwell donor had a three-fold greater volume-to-surface area ratio, resulting in less mixing and a thicker aqueous boundary layer. A fit of the binding expression defined in Fig. 4 gave an intrinsic partition coefficient (K_{intr}) of 3660 ± 130 between free CPZ in the aqueous solution and the cell and an apparent dissociation constant (k_d) of 4.0 ± 0.5 × 10^{-4} *M*. This value is an operational constant describing the BSA–CPZ interaction since the stoichiometry of this complex under these conditions was not determined. We examined the data with the assumption that the rate-limiting kinetic step in uptake was diffusion of both the free and the BSA-bound CPZ across the aqueous boundary layer (6), and not the subsequent partitioning step of free CPZ molecules into the outer leaflet of the AP membrane lipid bilayer and diffusion throughout the cell. There was a good linear relationship of the experimental data when the uptake P_e was plotted against the fraction of free CPZ concentration (Fig. 5), suggesting that uptake kinetics is aqueous boundary layer controlled.

Uptake of [^{3}H]CPZ by brain was measured in rats using the BUI method and an injectate consisting of 3% BSA in HBSS-HEPES, pH 7.4. Relative to the reference compound butanol, CPZ had an extraction efficiency of 87 ± 6% (mean ± SD; $n = 3$).

Efflux Kinetics

Because permeation of CPZ across MDCK cell monolayers was slow and the K_{intr} of CPZ into the cells was high, we examined efflux of cell-associated [^{3}H] CPZ as a function of BSA concentration. First, efflux from the AP membrane was measured in plastic-grown cell monolayers. The entire bathing solution was replaced to maintain sink conditions.

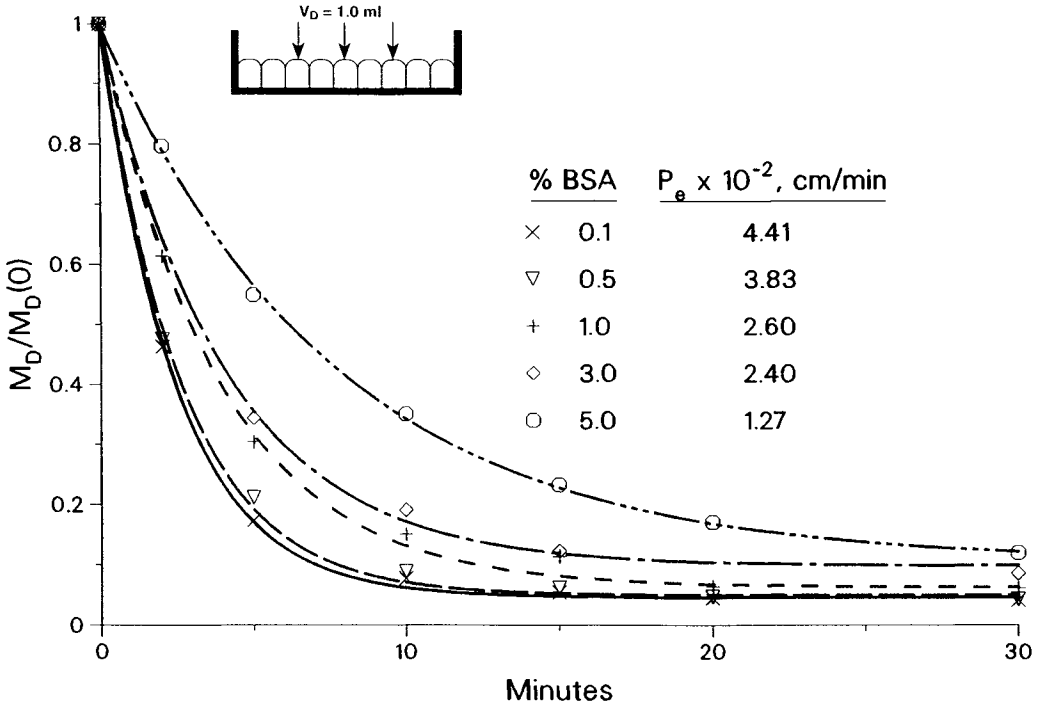

Fig. 3. Uptake kinetics of [^{3}H]CPZ measured as disappearance from the donor as a function of BSA concentration into MDCK cell monolayers grown on a plastic substrate. The details of the experiment are described under Materials and Methods. Data are the fraction of mass in the donor at time t (M_D) relative to the mass in the donor at $t = 0$ [$M_D(0)$]. Standard deviations ($n = 3$) are <5% of the mean, and the mass balance was ~100%. The experiment was continued for 2 hr and the residual M_D remained constant (not shown).

As expected, the rate of efflux was increased slightly with increases in BSA concentration (Fig. 6).

Apical membrane efflux was compared to efflux of cell-associated CPZ from the BL membrane. The rate of desorption of radioactivity into the BL receiver from filter-grown cell monolayers, previously equilibrated with [^{3}H]CPZ, was measured. After loading, the cells were rinsed and the donor solution was completely removed except for a thin film of buffer covering the cells to prevent drying. Although this creates a hydrostatic pressure against diffusion, the effect is trivial given the slow efflux rates of a molecule that diffuses transcellularly. The P_e values of BL efflux at 0.5% (0.9×10^{-6} cm min^{-1}) and 3% (2.4×10^{-6} cm min^{-1}) BSA compared well to those measured from the AP membrane (0.83 and 1.56×10^{-6} cm min^{-1}, respectively). The mass transport resistance of the microporous filter was insignificant and there was no apparent need to correct for the area of the BL membrane directly exposed to the pores of the filter.

DISCUSSION

This study attempts to understand the permeability of cellular barriers to lipophilic molecules by employing an *in vitro* cell culture model and kinetic analyses applied through a biophysical model described in detail elsewhere (7). Several key issues were concluded from this study. First, the results showed the importance of following donor disappearance in addition to receiver appearance under conditions where cell accumulation is significant. We showed that the kinetics of appearance, which are used to derive the apparent permeability, were independent of the disappearance kinetics. Second, the data showed that permeability or appearance in the receiver is membrane controlled despite appreciable water solubility and is dependent upon the nature of the acceptor in the receiver. Third, this dependence of permeability upon the receiver environment raised the issue of how well the *in vitro* model with a predominantly aqueous receiver predicts permeability *in vivo* and, more importantly, penetration into underlying tissues.

Cell (Membrane) Partition Coefficient of CPZ

The model is partly validated by the comparison of our calculated parameters versus values that were measured independently. The K_{intr} of ~3700 reported here was similar to partition coefficients (K) of 2750 for isolated cell membrane fractions at pH 7.4 (14), and $K = 2700 \pm 300$ for erythrocyte ghosts at pH 7.4 (15). Our value was calculated using the total cell volume, whereas the other values were obtained using only membranes; therefore, if CPZ partitions into cell cytoplasm consisting of intracellular membranes, proteins, and lipid deposits, then we might expect to see a slightly larger K_{intr}. Access of lipophilic compounds into cytoplasmic sites has not been well defined experimentally. It is probable that, despite the high K_{intr} value of CPZ for membranes, CPZ could be delivered to intracellular membranes through its association with cytoplasmic proteins, especially since it is available at the cytoplasmic face of the plasma membrane (4). Using a precipitation technique to visualize drugs within tissues, it was suggested that CPZ located in intracellular

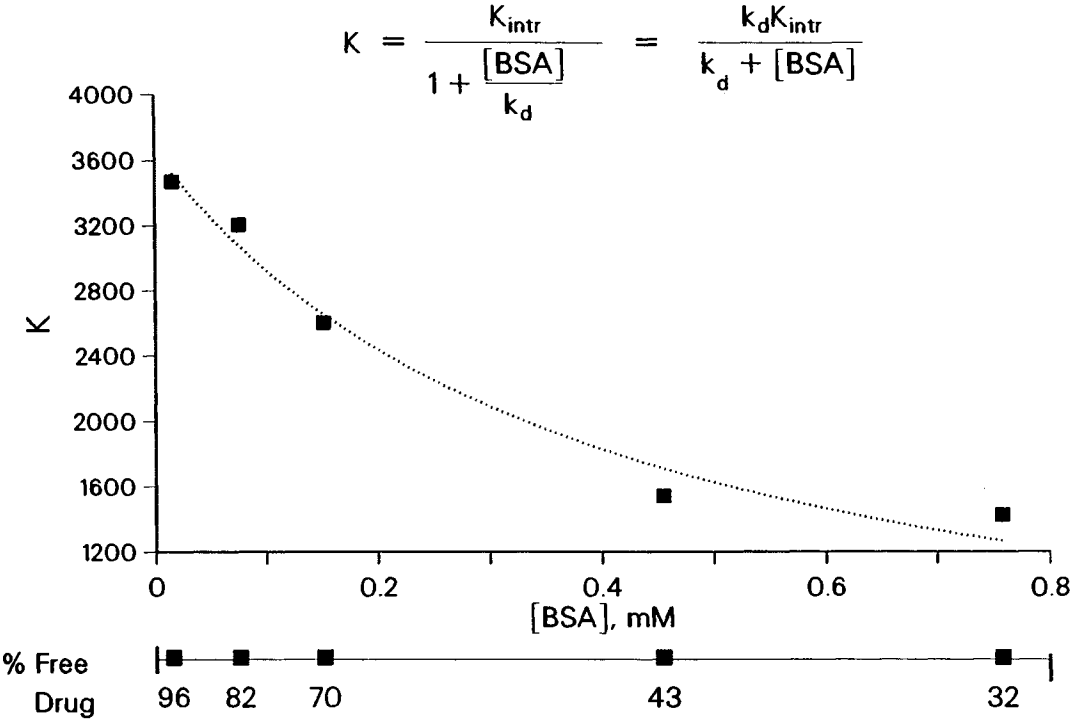

Fig. 4. The apparent membrane partition coefficient of [^{3}H]CPZ as a function of molar concentration of BSA and free CPZ concentration. K_{intr} (mean ± SD) was calculated from the curve fit to the uptake data (Fig. 3) using the equation shown. The binding constants are operational constants since the stoichiometry of the BSA–CPZ complex was not explicitly determined.

membranes (16); however, this method remains to be validated.

Binding Constants of CPZ for BSA

Our estimated k_d of 4×10^{-4} *M* for BSA binding of CPZ from the uptake kinetics compares to the 0.5×10^{-4} *M* measured directly using fatty acid-containing BSA (17). The difference between these values might be attributed to the use of a cell system versus a protein–ligand assay much in the same way that k_d values measured *in vivo* are nearly an order of magnitude greater than those measured *in vitro* (1). It is equally possible that the difference in k_a values was caused by variations in BSA and fatty acid content. The accuracy of k_d values measured *in vitro* appeared complicated by the variability in the number of binding sites on albumin for CPZ, which ranges from 1 to >3 depending upon the albumin concentration (18). Therefore, we emphasize that our estimate of the binding constant is an operational value at best, requiring further confirmation using this approach.

Permeability and the Interplay of Various Factors

The kinetics of permeation of very lipophilic molecules across cellular barriers involves an interplay of membrane partitioning, protein binding, and aqueous solubility. We previously examined transmonolayer flux of two other very lipophilic molecules in this model (7) and compare the results in Table I. The K_{intr} of CPZ is $>10^3$ larger than that measured for either of the lipophilic antioxidants, U-78517 or U-74006, even though these compounds have calculated log-$PC_{(n\text{-octanol/water})}$ values of >8. It is likely that this difference

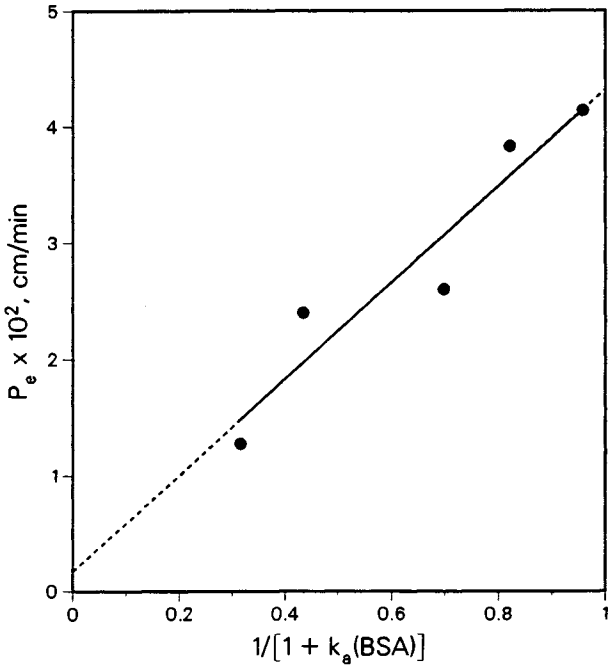

Fig. 5. Influence of free CPZ fraction on the effective permeability coefficients (P_e) determined from the kinetics of disappearance of [^{3}H]CPZ from the donor (Fig. 3), i.e., cell uptake of [^{3}H]CPZ. Linear regression gave a correlation $R^2 = 0.91$. The extrapolated intercepts are the permeability coefficients for free CPZ and the CPZ–BSA complex across the aqueous boundary layer.

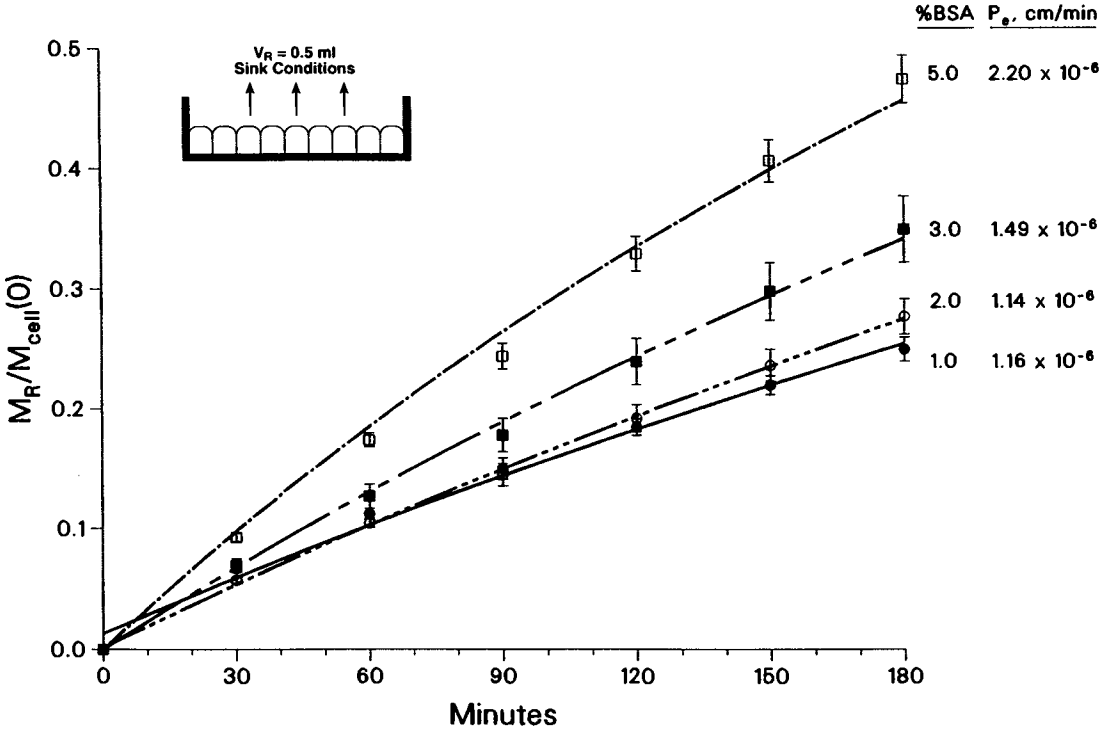

Fig. 6. Efflux kinetics of [^{3}H]CPZ from the apical surface of plastic-grown cell monolayers as a function of BSA concentration. Cell monolayers were allowed to equilibrate with [^{3}H]CPZ, then quickly rinsed in buffer, and loss of cell-associated radioactivity was measured with time under sink conditions. The data are the mass fraction of CPZ appearing in the receiver (M_R) versus the amount in the cell at $t = 0$ [$M_D(0)$]. Curve fitting was done using Eqs. (1) and (2). Standard deviations ($n = 3$) were <5% of the mean and the mass balance was ~100%.

in K_{intr} is because CPZ, which is a stronger base than the antioxidants, with pK's of ~6 to 7, has stronger ionic interactions with membrane components. For example, the calcium-channel antagonist amlodipine, with a pK_a of ~9, is highly partitioned into the membrane most likely because of ionic interactions with phospholipid headgroups (19). It has been suggested that lipophilic cations such as CPZ interact with negatively charged phosphatidylserine, which is at higher concentrations on the inner membrane bilayer leaflet (20). We also cannot rule out that binding of CPZ to membrane proteins plays a significant role in partitioning (21). In addition to the difference in K_{intr}, U-78517 and U-74006 have 5- and 33-fold, respectively, stronger apparent affinities for BSA, resulting in lower free drug concentrations (Table I). The combination of a larger K_{intr} and lower affinity for BSA results in a ~6- to 9-fold slower efflux P_e for CPZ, despite its having an aqueous solubility at pH 7.4 that is at least 6 × 10^3-fold greater than either of the antioxidants (Table I). Therefore, transmonolayer permeability of CPZ is mostly membrane limited or dependent upon the receiver-side environment, whereas not only are the antioxidants membrane limited, but also their permeability is dependent upon protein binding and subsequent cell accumulation from the donor side (7).

The Receiving Solution: Its Role in Permeability

The importance of the composition of the receiver solution in transcellular flux of membrane-limited molecules was emphasized by replacing BSA with α_1-AGP. α_1-AGP is a 40-kD plasma protein, at physiological concentrations of 14 to 37 μM in plasma (22), with a k_a for CPZ that is ~10^3-fold greater than BSA (23). The higher affinity of CPZ for α_1-AGP was sufficient at 25 μM under sink conditions to overcome K_{intr}-dependent desorption. This observation emphasizes the importance of providing a receiving environment that mimics the *in vivo* situation being modeled. Otherwise the observed permeability *in vitro* does not reflect permeability, and especially penetration beyond the initial cellular barrier, *in vivo*. It is important to realize, too, that *in vitro* measurements using individual proteins or mixtures of proteins do not necessarily mimic the importance of these interactions in the blood *in vivo* (24). Despite the ability of α_1-AGP to bind lipophilic cations with a high affinity, it does not appear to play a major role in the pharmacokinetics of these compounds (25). In part this is attributed to the relatively large binding capacities of albumin and lipoproteins in spite of their relatively low affinities (26).

This cell culture-biophysical model was designed to understand the permeability of membrane-interacting compounds at the blood–brain barrier (BBB) by passive diffusion independent of BBB-specific metabolism or transport. However, given the importance of the environment underlying the endothelial barrier in facilitating desorption and subsequent penetration, it is unclear what kind of environment should be provided in the receiver *in vitro* as an *in vivo* equivalent. Rosen and Tham (27) suggested that penetration of CPZ into the CNS is facilitated by its avidity for an unidentified CNS component by increasing the concentration

Table I. Comparison of Efflux Permeability Coefficients, Fractions of Drug Bound to BSA, Intrinsic Partition Coefficients, and Apparent Binding Constants Between CPZ and the Lipophilic Antioxidants U-78517F and U-74006F

	CPZ		U-78517F[a]		U-74006F[a]	
% BSA	P_{ap}[b]	% BSA bound[c]	P_{ap}	% BSA bound	P_{ap}	% BSA bound
0	0.3	0	0.8	0	—	—
0.1	0.3	4	5.2	18	6.0	59
0.5	0.4	18	5.4	52	8.2	88
1.0	0.8	30	6.8	68	11.1	94
2.0	1.0	47	10.8	81	—	—
3.0	1.3	57	14.1	87	14.9	98
5.0	1.8	68	19.3	92	—	—
K_{intr}[d]	3660 ± 130		2050 ± 130		1150 ± 250	
k_d (M)[d]	$4 \pm 0.05 \times 10^{-4}$		$0.71 \pm 0.10 \times 10^{-4}$		$0.1 \pm 0.04 \times 10^{-4}$	
S[e]	300 μg/mL		≪50 ng/mL		≪50 ng/mL	

[a] Data from Raub *et al.* (7).
[b] P_e values of efflux from AP membrane. Units $\times 10^{-6}$ cm min^{-1}.
[c] Calculated from uptake kinetics.
[d] Calculated from nonlinear least-squares curve fitting of a plot of the effective partition coefficient (K) versus molar concentration of BSA (see Fig. 4). K was calculated from uptake kinetics. The dissociation binding constant (k_d) was calculated from the relationship between K and the free drug concentration (7) (see Fig. 4).
[e] Aqueous solubility at pH 7.0 (5,7).

gradient from blood. Through fractionation they discounted albumin as an acceptor, and this is consistent with the low concentration of albumin in CSF (28). The tissue source of the binding sites apparently is not important since binding of CPZ to microsomes from a variety of different tissues including brain was equivalent (29). We examined the role of brain components by adding dilutions of rat brain homogenate to the buffer in experiments measuring P_{ap} efflux so that filter porosity did not limit access, but no effect on efflux kinetics was seen compared to BSA (G. A. Sawada and T. J. Raub, unpublished). Although the data shown here suggest that CPZ equilibration with underlying tissue could be slow, they also imply that conditions for equilibrium are favorable since accumulation by the cells that comprise the barrier is rapid and extensive.

Implications for Brain Uptake

What do these results predict for brain uptake *in vivo?* For the lipophilic antioxidants U-74006 and U-78517, brain uptake during first pass was very low, with extraction efficiencies of less than 10% (7). The model of Pardridge (30) attributes this to rates of dissociation (k_{off}) and/or uptake P_e that are much slower than the ~1-sec transit time. Both result in a low free drug concentration that is available to partition into the BBB endothelium (7). This was supported by a negative slope correlation between extraction efficiency of the antioxidants and concentration of protein in the injectate (T. J. Raub and L. R. Williams, unpublished). In contrast, brain uptake of CPZ from a bolus dose had an extraction efficiency of 87% under identical conditions. This *in vivo* measurement was consistent with a qualitative comparison to the rapid uptake P_e values for CPZ measured in our *in vitro* model, implying that the efficiency of brain uptake reflects the partitioning of CPZ into the BBB endothelium but not necessarily efflux (penetration) into the parenchyma. In other words, k_{off} of CPZ from BSA and uptake P_e were significantly faster than transit time (30). Because the lazaroids were not delivered efficiently to the BBB endothelium during first pass to create a sufficient concentration to drive a concentration gradient, subsequent diffusion into the CNS was further limited.

Obviously, distribution *in vivo* is much more complicated by the rate of clearance due to metabolism or nontarget tissue uptake. Brain partitioning will either increase or be sustained through continuous delivery for slowly cleared molecules or decrease as a result of brain-to-blood efflux as the vascular concentration of drug decreases. *In vitro* models like the one used here are not expected to predict bioavailability but are rather useful for manipulating the parameters that contribute to molecular permeation of cellular barriers.

ACKNOWLEDGMENTS

We thank Dr. Ferenc Kézdy, Biochemistry, Upjohn Laboratories, for helpful discussions and Dr. Phil Burton, Drug Delivery Systems Research, Upjohn Laboratories, for the HPLC analysis.

REFERENCES

1. W. M. Pardridge. Transport of plasma protein-bound drugs into tissues in vivo. In J.-P. Tillement and E. Lindenlaub (eds.), *Protein Binding and Drug Transport*, F. K. Schattauer Verlag, Stuttgart, 1986, pp. 277–292.
2. B. Fichtl, N. Alexander, and K. Walter. Tissue binding versus plasma binding of drugs: General principles and pharmacokinetic consequences. *Adv. Drug Res.* 20:117–166 (1991).

3. P. Seeman. The membrane actions of anesthetics and tranquilizers. *Pharmacol. Rev.* 24:583–655 (1972).
4. J. G. R. Elferink. The asymmetric distribution of chlorpromazine and its quaternary analogue over the erythrocyte membrane. *Biochem. Pharmacol.* 26:2411–2416 (1977).
5. A. T. Florence and D. Attwood. *Physiochemical Properties of Pharmacy,* Chapman and Hall, New York, 1981, p. 140.
6. S. H. Curry. Relationship between binding to plasma protein, apparent volume of distribution, and rate constants of disposition and elimination for chlorpromazine in three species. *J. Pharm. Pharmacol.* 24:818–819 (1972).
7. T. J. Raub, C. L. Barsuhn, L. R. Williams, D. E. Decker, G. A. Sawada, and N. F. H. Ho. Use of a biophysical-kinetic model to understand the roles of protein binding and membrane partitioning on passive diffusion of highly lipophilic molecules across cellular barriers. *J. Drug Target.* 1:269–286 (1993).
8. M. J. Cho, D. P. Thompson, C. T. Cramer, T. J. Vidmar, and J. F. Scieszka. The Madin Darby canine kidney (MDCK) epithelial cell monolayer as a model cellular transport barrier. *Pharm. Res.* 6:71–77 (1989).
9. Statistical Consultants, Inc. PCNONLIN and NONLIN84: Software for the statistical analysis of nonlinear models. *Am. Stat.* 40:No. 1 (1986).
10. W. H. Oldendorf. Clearance of radiolabeled substances by brain after arterial injection using a diffusible internal standard. *Res. Method Neurochem.* 5:91–112 (1981).
11. E. M. Cornford, D. Young, and J. W. Paxton. Comparison of the blood-brain barrier and liver penetration of acridine antitumor drugs. *Cancer Chemother. Pharmacol.* 29:439–444 (1992).
12. J. Folch, M. Lees, and G. H. Sloane-Stanley. A simple method for the isolation and purification of total lipids from animal tissues. *J. Biol. Chem.* 226:497–509 (1957).
13. J. W. Paxton. Alpha$_1$-acid glycoprotein and binding of basic drugs. *Method. Find. Exp. Clin. Pharmacol.* 5:635–648 (1983).
14. B. Bondy and J. Remien. Differential binding of chlorpromazine to human blood cells: Application of the hygroscopic desorption method. *Life Sci.* 28:441–449 (1981).
15. M. Luxnat and H.-J. Galla. Partition of chlorpromazine into lipid bilayer membranes: The effect of membrane structure and composition. *Biochim. Biophys. Acta* 856:274–282 (1986).
16. G. M. Grass and J. R. Robinson. Mechanisms of corneal drug penetration. II. Ultrastructural analysis of potential pathways for drug movement. *J. Pharm. Sci.* 77:15–23 (1988).
17. J. Krieglstein, W. Meiler, and J. Staab. Hydrophobic and ionic interactions of phenothiazine derivatives with bovine serum albumin. *Biochem. Pharmacol.* 21:985–997 (1972).
18. S. Gabay and P. C. Huang. The binding behavior of phenothiazines and structurally related compounds to albumin from several species. In I. S. Forrest, C. J. Carr, and E. Usdin (eds.), *The Phenothiazines and Structurally Related Drugs,* Raven Press, New York, 1974, pp. 175–189.
19. R. P. Mason, S. F. Campbell, S.-D. Wang, and L. G. Herbette. Comparison of location and binding for the positively charged 1,4-dihydropyridine calcium channel antagonist amlodipine with uncharged drugs of this class in cardiac membranes. *Mol. Pharmacol.* 36:634–640 (1989).
20. M. P. Scheetz and S. J. Singer. Biological membranes as bilayer couples. A molecular mechanism of drug-erythrocyte interactions. *Proc. Natl. Acad. Sci. USA* 71:4457–4461 (1974).
21. J. G. R. Elferink. Fluorescence studies of membrane interactions of chlorpromazine and chlorimipramine. *Biochem. Pharmacol.* 26:511–515 (1977).
22. P. Lunde, E. Pike, and J. E. Bredsen. Inflammation and alpha$_1$-acid glycoprotein: Effect on drug binding. In M. M. Reidenberg and S. Erill (eds.), *Drug-Protein Binding,* Praeger Scientific, New York, 1984, pp. 201–219.
23. W. E. Müller and A. E. Stillbauer. Characterization of a common binding site for basic drugs on human α_1-acid glycoprotein (orosomucoid). *Naunyn-Schmied. Arch. Pharmacol.* 322:170–173 (1983).
24. R. K. Verbeeck, J.-A. Cardinal, A. G. Hill, and K. K. Midha. Binding of phenothiazine neuroleptics to plasma proteins. *Biochem. Pharmacol.* 32:2565–2570 (1983).
25. W. E. Müller, S. Rick, and F. Brunner. Drug binding to human α_1-acid glycoprotein focus on a single binding site. In J.-P. Tillement and E. Lindenlaub (eds.), *Protein Binding and Drug Transport,* F. K. Schattauer Verlag, Stuttgart, 1986, pp. 29–44.
26. S. Urien. Interaction of drugs with human plasma lipoproteins. In J.-P. Tillement and E. Lindenlaub (eds.), *Protein Binding and Drug Transport,* F. K. Schattauer Verlag, Stuttgart, 1986, pp. 63–75.
27. A. Rosen and S. Y. Tham. The binding of chlorpromazine to some fractions of homogenized rat brain. *J. Pharm. Pharmacol.* 32:357–359 (1980).
28. H. Davson, K. Welch, and M. B. Segal. *Physiology and Pathophysiology of the Cerebrospinal Fluid,* Churchill Livingstone, Edinburgh, 1987.
29. M. H. Bickel. Binding of phenothiazines and related compounds to tissues and cell constituents. In I. S. Forrest, C. J. Carr, and E. Usdin (eds.), *The Phenothiazines and Structurally Related Drugs,* Raven Press, New York, 1974, pp. 163–166.
30. W. M. Pardridge. Transport of protein-bound hormones into tissues *in vivo. Endocrine Rev.* 2:103–123 (1981).